JACS
JOURNAL OF THE AMERICAN CHEMICAL SOCIETY
Article
pubs.acs.org/JACS

Polymorphic Phases of sp^3-Hybridized Carbon under Cold Compression

Rulong Zhou[†,‡] and Xiao Cheng Zeng*[,†]

[†]Department of Chemistry and Nebraska Center for Materials and Nanoscience, University of Nebraska—Lincoln, Lincoln, Nebraska 68588, United States

[‡]School of Science and Engineering of Materials, Hefei University of Technology, Hefei, Anhui 230009, China

Supporting Information

ABSTRACT: It is well established that graphite can be transformed into superhard carbons under cold compression (Mao et al. *Science* **2003**, *302*, 425). However, structure of the superhard carbon is yet to be determined experimentally. We have performed an extensive structural search for the high-pressure crystalline phases of carbon using the evolutionary algorithm. Nine low-energy polymorphic structures of sp^3-hybridized carbon result from the unbiased search. These new polymorphic carbon structures together with previously reported low-energy sp^3-hybridized carbon structures (e.g., M-carbon, W-carbon, and Cco-C_8 or Z-carbon) can be classified into three groups on the basis of different ways of stacking two (or more) out of five (A−E) types of buckled graphene layers. Such a classification scheme points out a simple way to construct a variety of sp^3-hybridized carbon allotropes via stacking buckled graphene layers in different combinations of the A−E types by design. Density-functional theory calculations indicate that, among the nine low-energy crystalline structures, seven are energetically more favorable than the previously reported most stable crystalline structure (i.e., Cco-C_8 or Z-carbon) in the pressure range 0−25 GPa. Moreover, several newly predicted polymorphic sp^3-hybridized carbon structures possess elastic moduli and hardness close to those of the cubic diamond. In particular, Z-carbon-4 possesses the highest hardness (93.4) among all the low-energy sp^3-hybridized carbon structures predicted today. The calculated electronic structures suggest that most polymorphic carbon structures are optically transparent. The simulated X-ray diffraction (XRD) spectra of a few polymorphic structures are in good agreement with the experimental spectrum, suggesting that samples from the cold-compressed graphite experiments may consist of multiple polymorphic phases of sp^3-hybridized carbon.

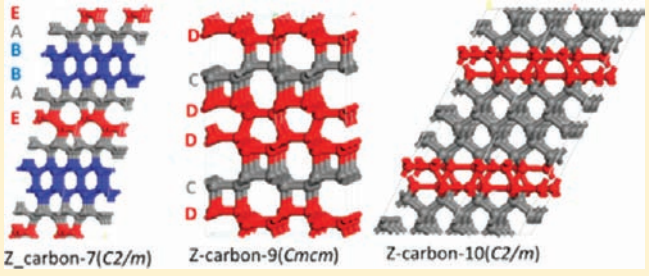

INTRODUCTION

Carbon, one of cornerstone elements in organic and biochemistry, is known to possess rich allotropic structures owing to its unique capability to form sp-, sp^2-, and sp^3-hybridized bonds. Low-dimensional allotropic structures of carbon include zero-dimensional (0D) fullerenes, 1D carbon nanotubes, and 2D graphene sheets. Moreover, carbon also exhibits rich 3D polymorphic structures at ambient pressure, such as the graphite, cubic diamond, and hexagonal diamond (lonsdaleite). The latter forms, typically, when meteorites containing graphite collide the earth.[1−3] Among the known 3D crystalline structures of carbon, the sp^2-hybridized carbon graphite is the most stable at ambient pressure, whereas the sp^3-hybridized cubic diamond is a metastable phase. At a high pressure (∼15 GPa) and high temperatures (1600−2500 K), graphite can be transformed into the cubic diamond.[4,5] On the other hand, at room temperature and high pressures (10−25 GPa), i.e., the so-called cold compression conditions, previous experiments have shown that the graphite can be converted into new 3D crystalline phases with distinctive properties including marked increases of electrical resistivity[6,7] and optical transmittance,[8,9] a significant decrease of the optical reflectivity,[10] as well as notable changes in near K-edge spectra, X-ray diffraction (XRD),[11−13] and Raman modes.[8,14,15] Moreover, the new phases of cold-compressed graphite are superhard due to their capability of indenting the cubic diamond.

Inspired by the experimental findings, much theoretical effort has been made to predict crystalline structures of the superhard carbon materials. Over the past two years, in particular, several low-energy polymorphic structures of sp^3-hybridized carbon have been reported in the literature, and are believed to entail higher stability than graphite at 20 GPa. These structures have been named, in the order of increasing stability: (1) the bct-C_4 structure found in a molecular dynamics study of compression of carbon nanotubes,[16] (2) the monoclinic M-carbon, obtained from an unbiased crystal structural search,[17] (3) the orthorhombic W-carbon,[18] (4) the hexagonal chiral C_6,[19] from a random structure search, and (5) the C-centered orthorhombic C_8 (Cco-C_8),[20a] or σC16−II,[20b] or Z-carbon.[20c] The latter carbon structure, which has three different names reported in the literature,[20] was independently revealed by

Received: February 16, 2012
Published: April 10, 2012

   dx.doi.org/10.1021/ja301582d | *J. Am. Chem. Soc.* 2012, 134, 7530−7538

three research groups from 2011 to 2012, using either an unbiased structural search, or the metadynamics simulation or the minimum-hopping method. The calculated transition pressures, bulk elastic moduli, and hardness, as well as the simulated XRD patterns of all five low-energy carbon polymorphs, are in good agreement with the experimental results, suggesting that all five polymorphic structures are potential structural candidates for the superhard carbon materials. Nevertheless, to date, detailed atomic structures of the cold-compressed graphite are still not fully resolved. The existence of multiple low-energy polymorphs of sp^3-hybridized carbon in the pressure range 10−25 GPa suggests that multiple crystalline phases may coexist in the experimental samples. Hence, more exhaustive structural searches are still needed to explore possible additional structural candidates for the superhard phases of cold-compressed graphite.

In this article, we present results of an extensive structural search of new polymorphic phases of carbon under high pressures based on the evolutionary algorithm combined with density functional theory (DFT) optimization. Besides some of the five low-energy polymorphic structures aforementioned, additional crystalline structures are also revealed, which are predicted to be more stable than graphite beyond the pressure of 10 GPa. The calculated elastic moduli and hardness suggest that these new crystalline phases belong to the group of superhard carbon materials. The calculated electronic band structures suggest that these crystalline phases are likely optical transparent. Finally, the simulated XRD patterns of some new crystalline phases are in good agreement with experiments.

COMPUTATIONAL METHODS

The search for crystalline structure of carbon at 15 GPa was performed using the USPEX package based on the evolutionary algorithm[21] which has successfully predicted several new high-pressure phases of various materials[21] and two-dimensional materials.[22] The evolutionary algorithm is one of the global optimization methods. Its development was inspired by the Darwinian evolution, which includes the concept of fitness, mating, and mutation. It has shown many successes in finding a large population of the local minima of clusters. The technique details of the evolutionary algorithm (or genetic algorithm) have been illustrated in ref 23. In the present structural search, 200 populations are generated randomly in the initial generation, and then 50 populations are generated according the evolutionary algorithm in the next generations. 60% populations in each generation are used to generate the offspring populations in the subsequent generation, which ensures good diversity in the populations of the offspring generations. Different separating schemes are employed in generating the initial populations to further increase the diversity of populations for large supercells. Four lowest-energy structures in each generation are kept to compete with the structures in the next generation. We have examined various numbers of C atoms per unit cell, including 4, 8, 12, 16, and 20, for the crystal-structure search. In each case, more than 5000 populations are explored. The exhaustive structural search for a given atomic-number per unit cell allows us to attain new low-energy polymorphic structures of carbon hitherto unreported in the literature.

The structural relaxation and total-energy calculation are performed using the VASP package[24] within the local density approximation (LDA). An energy cutoff of 520 eV and all-electron plane-wave basis sets within the projector augmented wave (PAW) method are chosen. A dense K-point sampling with the grid spacing less than $2\pi \times 0.02$ $Å^{-1}$ in the Brillouin zone is used. Phonon spectra of the low-energy crystalline structures are calculated (see Supporting Information Figure S1) using the VASP package combined with the PHONOPY program,[25] in order to ensure that the crystalline structures entail no negative phonon frequencies and the crystalline structures are metastable. The elastic moduli of the crystals are calculated on the basis of the stress tensor at different structural deformation and strains[26] using the VASP package. The hardness of the crystals is calculated using the Šimůnek's method.[27] The simulated XRD pattern is based on the REFLEX program implemented in Materials Studio 4.4 package.[28]

RESULTS AND DISCUSSION

1. Structures of Nine Newly Predicted Carbon Polymorphs. The structural search reproduces previously known sp^3-hybridized carbon structures, including the cubic diamond, hexagonal diamond, M-carbon, bct-C_4, and Cco-C_8 (σC16-II or Z-carbon) structures. Furthermore, the search gives rise to nine new low-energy crystalline structures of carbon, all having lower energies (or enthalpies) than graphite at pressure beyond 15 GPa. The calculated phonon spectra for all nine new carbon crystals indicate that these structures are locally stable without having negative phonon frequency (Figure S1). Most of the nine structures can be classified into one of the five (A−E) types of carbon layers according to different buckling mode of the graphene (see Figure 1).

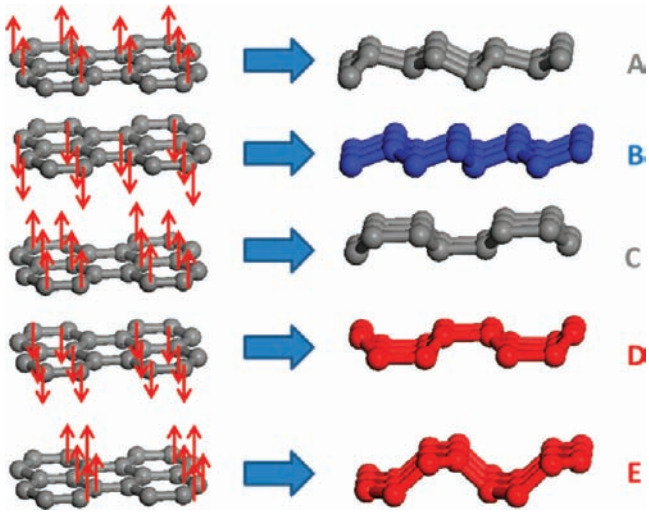

Figure 1. Five types of (periodic) carbon layer due to different buckling mode of the graphene. Each red arrow marks an out-of-plane direction for a single carbon atom.

The A- and B-type carbon layers (Figure 1) can be viewed as buckling of every carbon atom on every other straight line along the zigzag-chain direction. In other words, all carbon atoms on one sublattice of the graphene layer are moved upward while all carbon atoms on another sublattice are moved downward. Hence, each buckled carbon layer consists of chairlike 6-membered rings. The stacking of only A-type or B-type carbon layers (i.e., AA-stacking or BB-stacking) yields the cubic diamond structure, while the stacking of mixed A-type and B-type carbon layers can yield a variety of hexagonal and trigonal structures, e.g., the hexagonal diamond structure which can be viewed as the alternative stacking A- and B-type carbon layers (i.e., AB-stacking). The C- and D-type carbon layers can be viewed as buckling of every other two straight lines of carbon atoms (not on the same zigzag chain) along the zigzag-chain direction. Hence, each buckled carbon layer consists of saddle-like hexagonal rings. The alternative stacking of C- and D-type carbon layers (i.e., CD-stacking) yields the structure of bct-C_4. Lastly, the E-type carbon layer can also be viewed as buckling of every other zigzag chain of carbon atoms along the

dx.doi.org/10.1021/ja301582d | J. Am. Chem. Soc. 2012, 134, 7530−7538

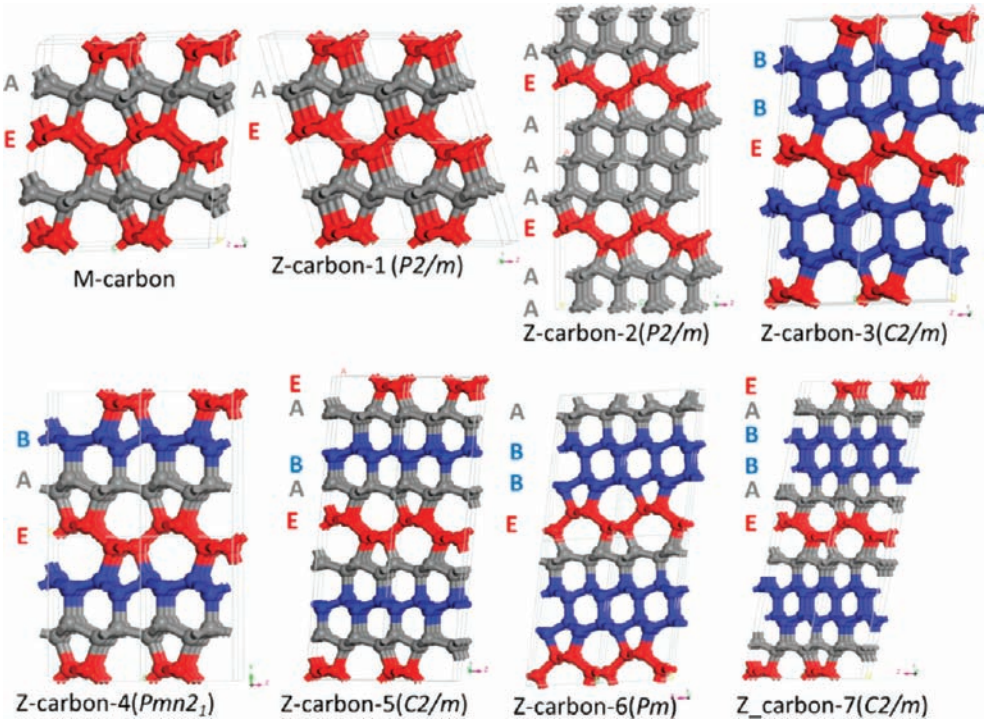

Figure 2. Polymorphic crystalline structures of carbon in group I: M-carbon and Z-carbon-1 to Z-carbon-7. Gray (A-type), red (E-type), and blue (B-type) highlight different types of carbon layers.

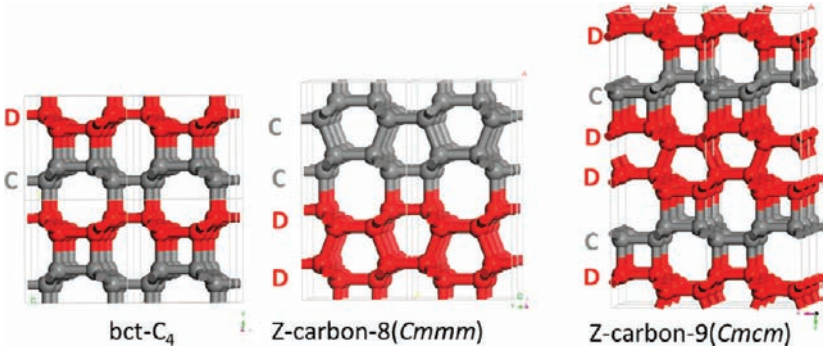

Figure 3. Three crystalline structures of carbon belonging to group II: Z-carbon-8, Z-carbon-9, and bct-C_4. Gray (C-type) and red (D-type) highlight different types of carbon layers.

zigzag-chain direction. The alternative stacking of E- and A-type carbon layers (i.e., EA-stacking) yields the structure of M-carbon[17] and W-carbon.[18a] Since each type of A−E carbon layers can be found in the known carbon structures or previously predicted carbon structures, they are all likely to exist in cold-compressed graphite and to form superhard carbon materials. Hence, multiple polymorphic crystalline phases composed of mixed carbon layers of A−E types are expected besides the known or previously predicted structures.

The nine new carbon structures, together with previously reported structures of M-carbon, bct-C_4, and Z-carbon-8, are displayed in Figures 2−4. Their designated crystal system, space group (No.), stacking pattern in the conventional cell, the number of atoms in one conventional cell (N_a), and the number of inequivalent crystallographic sites (N_i) are listed in Table 1. On the basis of different ways of stacking the carbon layers A−E, we classify these crystalline structures in three groups.

Group I includes seven new crystalline structures, namely, Z-carbon-1 to Z-carbon-7. All the seven structures can be viewed as stacking of the E-type carbon layers mixed with either the A-

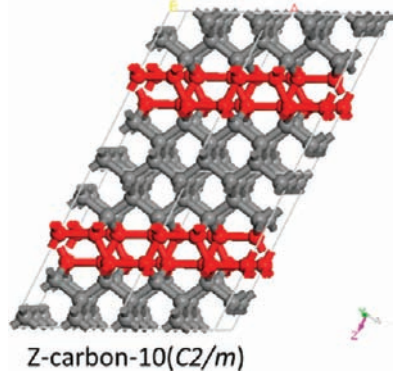

Figure 4. The only crystalline structure in the group III: Z-carbon-10.

dx.doi.org/10.1021/ja301582d | J. Am. Chem. Soc. 2012, 134, 7530−7538

Table 1. Designated Crystal System, Space Group (No.), Stacking Pattern in the Conventional Unit Cell, Number of Atoms in One Conventional Cell (N_a), and the Number of Inequivalent Crystallographic Sites (N_i) for Nine Newly Predicted Crystalline Structures,[a] and for Three Previously Reported Structures[b]

carbon structure	cryst syst	space group (No.)	stacking pattern	N_a	N_i
M-carbon	monoclinic	*C*2/*m* (12)	EAEA	16	4
bct-C_4	tetragonal	*I*4/*mmm* (139)	CDCD	8	1
Z-carbon-8	orthorhombic	*Cmmm* (65)	CCDDCCDD	16	2
Z-carbon-1	monoclinic	*P*2/*m* (10)	EAEA	8	4
Z-carbon-2	monoclinic	*P*2/*m* (10)	EAAAEAAA	16	8
Z-carbon-3	monoclinic	*C*2/*m* (12)	EBBEBB	24	6
Z-carbon-4	orthorhombic	*Pmn*2_1 (31)	EABEAB	12	6
Z-carbon-5	monoclinic	*C*2/*m* (12)	EABAEABA	32	8
Z-carbon-6	monoclinic	*Pm* (6)	EBBAEBBA	16	16
Z-carbon-7	monoclinic	*C*2/*m* (12)	EABBAEABBA	40	10
Z-carbon-9	orthorhombic	*Cmcm* (63)	CDDCDD	24	3
Z-carbon-10	monoclinic	*C*2/*m* (12)		32	6

[a]Z-carbon-1 to Z-carbon-7, Z-carbon-9, and Z-carbon-10. [b]M-carbon, bct-C_4 and Z-carbon-8.

type or B-type carbon layers. In addition, M-carbon belongs to group I. As shown in Figure 2, the combination of E-type carbon layer with A-type or B-type carbon layers introduces pentagon/heptagon pairs. It has been previously demonstrated that periodic pentagon/heptagon pairs can present in 2D carbon structures (known as haeckelite), which can result in novel electronic and mechanical properties.[29−32] However, the pentagon/heptagon pairs in the 3D carbon crystals are quite different from those formed in the haeckelite structures because they are not in the same plane but are buckled to connect with adjacent layers.

In Z-carbon-1, the stacking pattern of buckled carbon layers is EAEA, the same as that in M-carbon. The only difference between Z-carbon-1 and M-carbon is the relative position between the neighboring E-type layers. Hence, the enthalpies per atom for both crystalline structures at the same pressure are very close. Like M-carbon, Z-carbon-1 is a monoclinic crystal with the *P*2/*m* (SG No. 10) space group. A conventional unit cell of Z-carbon-1 contains 8 atoms with the lattice parameters of a = 4.676 Å, b = 2.474 Å, c = 4.043 Å, and β = 106.00° at 15 GPa. The four inequivalent crystallographic sites of Z-carbon-1 are (0.46522, 0, 0.16639), (0.11736, 0, 0.17416), (0.11252, 0.5, 0.39927), (0.57959, 0.5, 0.36767), respectively.

In Z-carbon-2, the stacking pattern of buckled carbon layers is EAAAEAAA. In a sense, Z-carbon-2 can be viewed as a superlattice of a bilayer M-carbon (AEA-stacking) and a bilayer of cubic diamond (AAA-stacking). Because the cubic diamond structure is more stable than M-carbon within a pressure range 10−25 GPa, it is not surprising that Z-carbon-2 is more stable than M-carbon in the same pressure range. A conventional unit cell of Z-carbon-2 contains 16 atoms with the lattice parameters of a = 8.489 Å, b = 2.475 Å, c = 4.177 Å, and β = 90.33° at 15 GPa. The eight inequivalent crystallographic sites of Z-carbon-2 are (0.27208, 0.5, 0.51176), (0.44142, 0.5, 0.63745), (0.97558, 0.5, 0.16911), (0.19825, 0.5, 0.83245), (0.26620, 0, 0.98791), (0.03543, 0, 0.33482), (0.55965, 0, 0.13796), (0.22026, 0, 0.33570), respectively.

In Z-carbon-3, the stacking pattern of buckled carbon layers is EBBEBB. The two adjacent B-type layers can be viewed as a single layer of cubic diamond (in BB-stacking). Hence, Z-carbon-3 can be viewed as a superlattice of a bilayer M-carbon with a single layer of cubic diamond. As expected, Z-carbon-3 is energetically more favorable than M-carbon, but slightly less favorable than Z-carbon-2. A conventional unit cell of Z-carbon-3 contains 24 atoms with the lattice parameters of a = 12.961 Å, b = 2.476 Å, c = 4.148 Å, and β = 96.37° at 15 GPa. The six inequivalent crystallographic sites of Z-carbon-3 are (−0.81824, 0, 0.22639), (−0.70041, 0, 0.26709), (−0.03932, 0, 0.34859), (−0.64947, 0, 0-.96242), (−0.53849, 0, 0.12529), (−0.15388, 0, 0.43514), respectively.

For Z-carbon-4 to Z-carbon-7, all crystals are composed of mixed E-, A-, and B-type carbon layers. In Z-carbon-4, the stacking pattern of buckled carbon layers is EABEAB in which the B-layer is slightly distorted. The adjacent A- and B-type layers can be viewed as a single layer of the hexagonal diamond (with AB-stacking). Thus, Z-carbon-4 can be viewed as a superlattice of a bilayer M-carbon with a single layer of hexagonal diamond. Because the hexagonal diamond is energetically more stable than M-carbon but slightly less stable than cubic diamond, it is expected that Z-carbon-4 is more stable than M-carbon but slightly less stable than Z-carbon-3. Contrary to other structures in group I, Z-carbon-4 is an orthorhombic crystal. A conventional unit cell of Z-carbon-4 contains 12 atoms with the lattice parameters of a = 12.961 Å, b = 2.476 Å, c = 4.148 Å, and β = 96.37° at 15 GPa. The six inequivalent crystallographic sites of Z-carbon-4 are (0, 0.29676, 0.53994), (0, 0.39966, 0.21745), (0, 0.92020, 0.68916), (0.5, 0.36261, 0.71758), (0.5, 0.30691, 0.06549), (0.5, 0.92429, 0.91317), respectively.

Z-carbon-5 can be viewed as inserting one A-type layer between the B and E layers in Z-carbon-4. Similarly, Z-carbon-6 can be viewed as inserting one B-type layer between B and A layers in Z-carbon-4. Z-carbon-7 can be constructed by inserting one A-type layer between E and B layers in Z-carbon-6. Therefore, the stacking patterns of Z-carbon-5 to Z-carbon-7 are EABAEABA, EBBAEBBA, and EABBAEABBA, respectively. All the three structures belong to monoclinic crystals. Z-carbon-5 and Z-carbon-6 can be also viewed as a superlattice of a bilayer M-carbon and a bilayer hexagonal diamond, while Z-carbon-7 can be viewed as a superlattice of a bilayer M-carbon and a trilayer of fused hexagonal and cubic diamond. As such, it is expected that the energetic stability increases from Z-carbon-5 to Z-carbon-7.

All crystalline structures in group II can be viewed as stacking of mixed C-type and D-type carbon layers. The simplest structure is the known structure of bct-C_4 with four-/eight-membered rings, which exhibits the stacking pattern of CDCD. Besides reproducing bct-C_4, the structure of previously predicted orthorhombic Cco-C_8[20a] or σC16−II[20b] or Z-carbon[20c] is also reproduced, which is named as Z-carbon-8 here. In Z-carbon-8, the stacking pattern is CCDDCCDD. The adjacent C- and D-type layers can be viewed as a single layer of bct-C_4, whereas the adjacent D- and D-type, or C- and C-type, layers can be viewed as a single layer of hexagonal diamond. Hence, Z-carbon-8 can be viewed as a superlattice of a single layer of bct-C_4 and a single layer of hexagonal diamond. Consequently, Z-carbon-8 is energetically much more stable than bct-C_4.[16] A conventional unit cell of Z-carbon-8 contains 16 atoms with the lattice parameters of a = 8.585 Å, b = 4.165 Å, c = 2.463 Å at 15 GPa. The two inequivalent crystallographic

dx.doi.org/10.1021/ja301582d | J. Am. Chem. Soc. 2012, 134, 7530−7538

sites are (−0.58926, −0.18512, 0.5) and (−0.33332, −0.31525, 0).

A new member of group II is the orthorhombic Z-carbon-9 whose stacking pattern of carbon layers is CDDCDD. Comparing to Z-carbon-8, there exist two bct-C_4 layers between the hexagonal diamond layers in Z-carbon-9. Because the bct-C_4 is notably less stable than hexagonal diamond, more bct-C_4 layers imply less stability of Z-carbon-9 than Z-carbon-8. A conventional cell of Z-carbon-9 contains 24 atoms with the lattice parameters of a = 2.4637 Å, b = 12.8806 Å, and c = 4.1999 Å. The three inequivalent crystallographic sites are (0, 0.60692, 0.06576), (0, 0.72638, 0.43207), and (0, 0.94443, 0.43479), respectively.

Finally, a unique crystalline structure (named as Z-carbon-10), significantly different from those of Z-carbon-1 to Z-carbon-9, is identified. This newly predicted structure is monoclinic and belongs to a new group (group III). As shown in Figure 4, apart from the red portion, the other portions (gray) exhibit perfect cubic-diamond structure. The red portion can be viewed as a stacking fault in the cubic-diamond structure. The two parallel C−C bonds (along the z-direction) in every hexagonal ring in the carbon layers of diamond sections become nonparallel in the stacking fault sections. This stacking fault weakens the structural stability of Z-carbon-10, compared to the cubic diamond. Thus, it is expected that Z-carbon-10 is less stable than most polymorphic structures in group I, except M-carbon and Z-carbon-1, but more stable than all polymorphic structures in group II in the pressure range considered in this study. A conventional cell of Z-carbon-10 contains 32 atoms with the lattice parameters of a = 4.796 Å, b = 4.941 Å, c = 8.245 Å, and β = 115.85° at 15 GPa. The six inequivalent crystallographic sites are (−0.49198, 0.23986, −0.82244), (−0.34900, −0.25042, −0.29876), (−0.07722, 0, −0.93789), (−0.63843, 0, −0.58970), (−0.58348, 0, −0.94288), (−0.00401, 0, −0.41038), respectively.

2. Relative Stabilities of Polymorphic Phases of sp^3-Hybridized Carbon. To assess relative stabilities of newly predicted polymorphic phases of carbon with respect to the graphite, relative enthalpies (at zero temperature) of the nine new crystalline structures are calculated with respect to the graphite in the pressure range 0−25 GPa (see Figure 5). Note that the zero-point energy (ZPE) corrections are not included in the enthalpy calculations. As shown in Figure 5, except for Z-carbo-1 the enthalpies of the other structures at 15 GPa are notably lower than that of the M-carbon (by ∼30−100 meV per atom in cohesive energy). Since the difference in ZPE between two structures is typically less than 5 meV, it is expected that the ZPE correction may change the relative stability between Z-carbon-1 and M-carbon, or relative stabilities among some of the structures from Z-carbon-2 to Z-carbon-10, but the relative stabilities between the M-carbon and any of the structures from Z-carbon-2 to Z-carbon-10 will not be affected qualitatively.

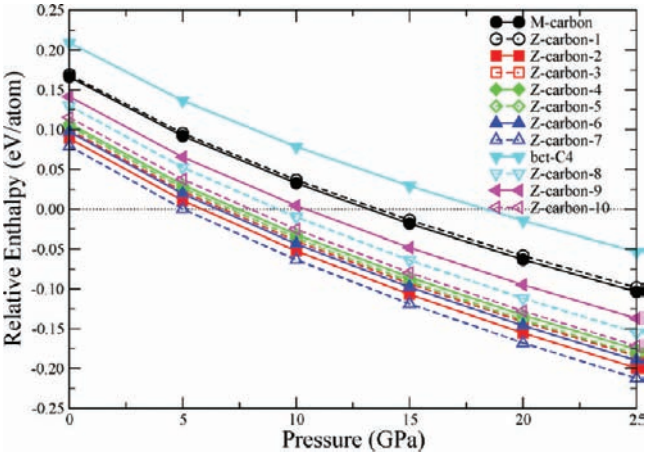

Figure 5. Calculated relative enthalpies of nine new crystalline structures, as well as those of M-carbon and bct-C4, with respect to the graphite (denoted by the dotted line) in the pressure range 0−25 GPa.

As shown in Figure 5, when sorted according to relative enthalpy starting from the lowest one, the polymorph structures in group I are Z-carbon-7, Z-carbon-2, Z-carbon-6, Z-carbon-3, Z-carbon-5, Z-carbon-4, Z-carbon-1. Note that the number of cubic-diamond or hexagonal-diamond fragmental layers (i.e., AA-, BB-stacking or AB-stacking layers) in these structures is 3, 2, 2, 1, 2, 1, 0 per E-type layer, respectively. This observation suggests that with inclusion of more cubic-diamond or hexagonal-diamond fragmental layers for group-I structures, higher stability is expected. Note also that the slightly higher stability of Z-carbon-3 over Z-carbon-5 is likely due to the higher stability of the cubic-diamond fragments over the hexagonal-diamond fragments. The same trend in relative stability can be also seen in group-II structures. In bct-C_4, there is no hexagonal-diamond fragment. In Z-carbon-8, the ratio of the hexagonal-diamond fragmental layers to the bct-C_4 layers is 1:1, while in Z-carbon-9 the ratio is 1:2. These results explain why Z-carbon-8 is the most stable, while bct-C_4 is the least among the three structures in group II.

On the basis of Figure 5, we can estimate the critical pressure P_c at which a crystalline phase becomes energetically more favorable than graphite. The P_c of Z-carbon-1 to Z-carbon-7, Z-carbon-9, and Z-carbon-10 are 13.6, 5.9, 6.8, 7.5, 7.1, 6.6, 5.1, 10.5, and 8.0 GPa, respectively. Note that although the critical pressures for most structures are below 10 GPa, these structures, if exist in nature, may be formed by compressing the graphite at much higher pressure than 10 GPa to overcome the energy barrier for the structural transition. Wang et al.[18a,b] estimated transition barriers from graphite to the M-carbon, W-carbon, bct-C_4, cubic diamond, and hexagonal diamond, respectively. They showed that the transition barrier from the graphite to W-carbon or to M-carbon is lower than that to the cubic diamond or to the hexagonal diamond, at relatively low pressure, but higher at relatively high pressure. On the basis of their calculations of energy barriers, we speculate that the transition barriers from the graphite to each polymorphic phase of Z-carbon-2 to Z-carbon-7 are likely lower than those from the graphite to M-carbon or to Z-carbon-1 at relatively high pressure, because Z-carbon-2 to Z-carbon-7 all entail certain structural features of the cubic diamond or hexagonal diamond. If so, although the critical pressures for Z-carbon-2 to Z-carbon-7 are much lower than those for the M-carbon and Z-carbon-1, the structural transition from the graphite to any of the polymorphic phases of Z-carbon-2 to Z-carbon-7 may occur at higher pressure than to the M-carbon or Z-carbon-1. Likewise, because the transition barrier from the graphite to hexagonal diamond is lower than that from the graphite to bct-C_4, we speculate that Z-carbon-8 and Z-carbon-9 may be formed at a lower pressure prior to the formation of bct-C_4. It is possible that, in the cold-compression experiments, many polymorphic

dx.doi.org/10.1021/ja301582d | J. Am. Chem. Soc. 2012, 134, 7530−7538

Table 2. Calculated Elastic Constant, Bulk Moduli (B_0), Hardness (H), and Electronic Band Gap (E_g) of the Newly Predicted and Previously Known Polymorphic Structures of Carbon

	elastic constants (GPa)											
crystal structure	C_{11}	C_{22}	C_{33}	C_{12}	C_{13}	C_{23}	C_{44}	C_{55}	C_{66}	B_0 (GPa)	H (GPa)	E_g (eV)
cubic diamond	1101	1101	1101	150	150	150	591	591	591	467	95.4	
M-carbon	977	1152	1096	58	183	102	545	473	398	435	89.6	3.57
bct-C_4	981	981	1259	192	75	75	465	465	316	434	91.8	2.93
Z-carbon-8	1173	1132	1253	88	40	107	523	470	366	448	91.3	4.09
Z-carbon-1	1023	1146	1093	50	141	110	503	443	398	429	66.7	4.54
Z-carbon-2	1082	1175	1169	65	116	112	543	474	436	446	92.4	4.41
Z-carbon-3	1021	1163	1154	66	147	111	537	474	421	443	92.6	5.27
Z-carbon-4	1173	1048	1163	57	111	134	470	546	412	443	93.5	4.60
Z-carbon-5	1134	1196	1188	43	93	111	550	459	421	446	34.1	4.17
Z-carbon-6	1109	1183	1182	55	103	112	544	463	427	446	34.2	4.61
Z-carbon-7	1139	1204	1197	51	88	114	547	468	430	450	89.2	4.47
Z-carbon-9	1255	1075	1091	100	51	127	349	470	505	442	90.2	2.86
Z-carbon-10	1118	1144	1119	55	122	125	527	498	444	443	88.1	4.24

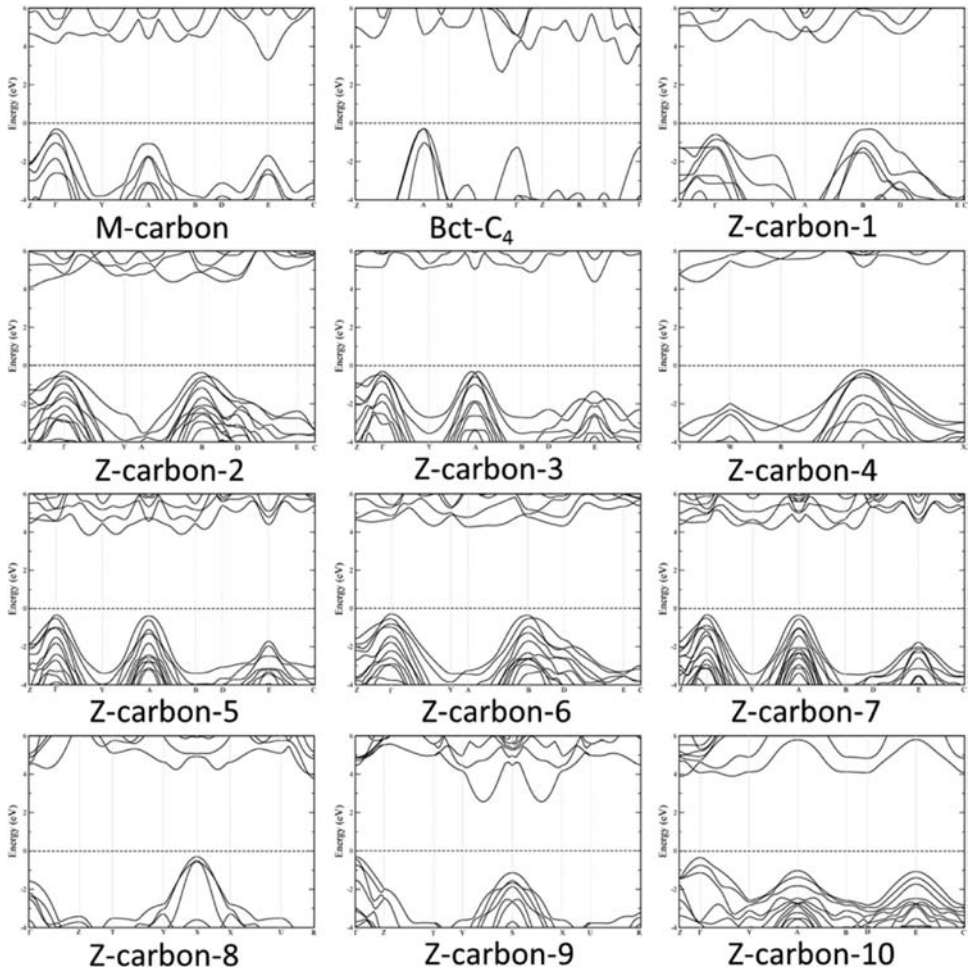

Figure 6. Calculated electronic band structures of nine new structures: Z-carbon-1 to Z-carbon-7, Z-carbon-9, and Z-carbon-10, as well as those of M-carbon, bct-C_4, and Z-carbon-8.

structures may coexist in the samples due to their similarity in structures and closeness in enthalpy.

3. Mechanical and Electronic Properties. It is known that the cold-compressed graphite is superhard with comparable hardness as the cubic diamond. We have calculated elastic constants and hardness of the nine newly predicted crystalline structures, together with three previously known crystalline structures (see Table 2). The principle elastic constants C_{11}, C_{22}, and C_{33} of all new structures are greater than 1 TPa, close to those of the cubic diamond. Hence, these newly predicted crystalline structures would possess comparable Young's moduli in the *x*-, *y*-, and *z*-directions as the cubic diamond. Other than Z-carbon-1, the bulk moduli of all nine structures are about 10 GPa higher than those of the M-carbon

dx.doi.org/10.1021/ja301582d | J. Am. Chem. Soc. 2012, 134, 7530−7538

and bct-C_4, and about 20 GPa lower than that of the cubic diamond. Among the nine structures, Z-carbon-7 has the highest bulk modulus. The presence of either cubic diamond or hexagonal diamond layers in the structures of Z-carbon-2 to Z-carbon-10 is responsible to their higher bulk moduli compared to the M-carbon. The calculated hardness indicates that, other than Z-carbon-5 and Z-carbon-6, other crystalline structures belong to the superhard materials. Among these superhard structures, Z-carbon-4 possesses the highest hardness, closest to that of the cubic diamond. The hardness of Z-carbon-7 and Z-carbon-9 is very close to that of bct-C_4 and Z-carbon-8. The relative low hardness of Z-carbon-5 and Z-carbon-6 is due to the elongated C−C bonds connecting the A-type and B-type carbon layers in both structures.

Previous experiments also showed that the cold-compressed graphite is optically transparent. We have computed electronic band structures of all nine structures (with lattice constants obtained at pressure of 15 GPa), as shown in Figure 6. The calculated band gaps are listed in Table 2. Other than Z-carbon-9, the band gaps of eight new structures are all greater than 4 eV, on the basis of LDA calculations. It is known that LDA calculations always underestimate the band gaps of semiconductors. In principle, the band gaps of these new structures should be larger. Therefore, except Z-carbon-9, the remaining eight structures should be optically transparent. In particular, the band gaps of the group I structures (Z-carbon-1 to Z-carbon-7) are notably larger than that of the M-carbon (also a member in group I). For structures in group II, Z-carbon-8 possesses a much larger band gap than bct-C_4 and Z-carbon-9. Umemoto et al.[16a] have shown that the band gap of bct-C_4 can be significantly increased (by more than 1.0 eV) if the GW approximation is used, which should be closer to the measured band gap of cold-compressed graphite. As such, the bct-C_4 could be optically transparent as well. Moreover, as shown in Figure 6, all nine new structures possess indirect band gaps, suggesting that electronic excitation is more difficult to achieve even if the optical energy matches the value of band gaps.

4. Simulated XRD Patterns. Finally, we present simulated XRD patterns of the nine new structures (at pressures 18.4 and 23.9 GPa, respectively) in Figure 7. Note that, in the experimental XRD spectra, the first strong peak at $2\theta \approx 7°$ corresponds to the diffraction from the (002) crystalline plane of the graphite, where θ is the diffraction angle. Other broad peaks arise in the range $2\theta \approx 9–10°$ and $15–16°$ at 23.9 GPa, while a small peak arises in the range $2\theta \approx 16.5–17°$ at 23.9 GPa. The two broad peaks might be contributed by different crystalline structures rather than a single crystalline structure. The simulated XRD patterns of several new crystals appear to be in reasonably good agreement with the experimental data as the strongest peak in many simulated XRD patterns is located between $2\theta \approx 9$ and 10°. Overall, the XRD patterns of Z-carbon-6, Z-carbon-7, and Z-carbon-9 appear to be in better agreement with the measured XRD as multiple peaks found between $2\theta \approx 9$ and 10° and between $2\theta \approx 15$ and 17° are gradually lowered from 18.4 to 23.9 GPa. Also, an overlap of the XRD patterns will result in two major broad peaks in the range $2\theta \approx 9–10°$ and $15–16°$, respectively, in good agreement with the experimental XRD spectra (at 18.4 and 23.9 GPa).[11]

5. Construction of New Carbon Polymorphs by Periodically Stacking Buckled Graphene Layers. The generic structural classification obtained from this study allows us to construct new low-energy sp^3-hybridized carbon allotrope structures via stacking buckled graphene layers in different

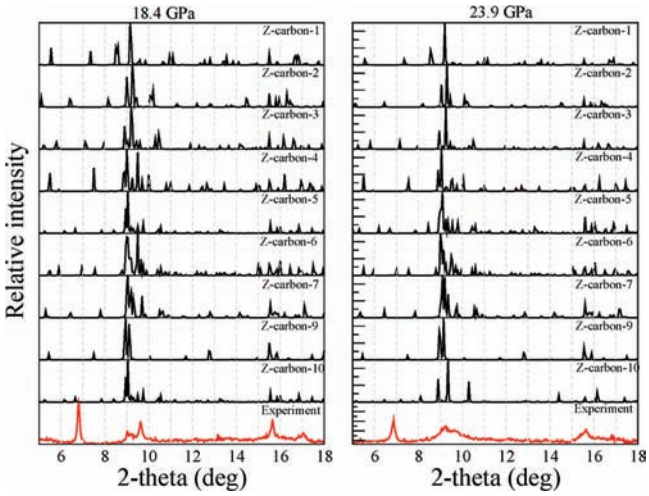

Figure 7. Simulated XRD patterns of nine newly predicted carbon structures at 18.4 and 23.9 GPa, respectively, as well as the experimental XRD pattern (in red).[11] The first strong peak at $2\theta \approx 7°$ corresponds to the diffraction from the (002) crystalline plane of the graphite. Here, θ is the diffraction angle.

combinations of the A−E types by design. As a proof of principle, we construct two structures (named as Z-carbon-11 and Z-carbon-12) by inserting more A-type and B-type buckled graphene layers into the structure of Z-carbon-4 and Z-carbon-5, respectively. The two new structures are shown in Figure 8a. Z-carbon-11 has a stacking pattern of ABABAE−ABABAE, and Z-carbon-12 has a stacking pattern of BABABAE−BABABAE. Indeed, both handmade structures are lower in energy than Z-carbon-7 (the lowest-energy structure obtained from the

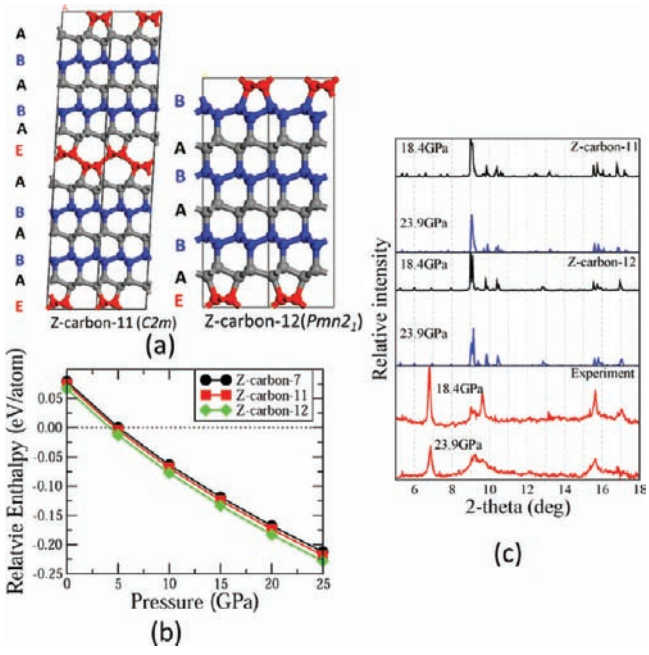

Figure 8. (a) Two handmade structures (Z-carbon-11 and Z-carbon-12), one by inserting one A- and one B-type buckled graphene layers in Z-carbon-5, and another by inserting two A- and two B- type layers in Z-carbon-4. (b) Relative enthalpies of Z-carbon-11 and Z-carbon-12 with respect to graphite, compared to Z-carbon-7. (c) Comparison of simulated XRD spectra of Z-carbon-11 and Z-carbon-12 with the experimental spectrum (red).

dx.doi.org/10.1021/ja301582d | J. Am. Chem. Soc. 2012, 134, 7530−7538

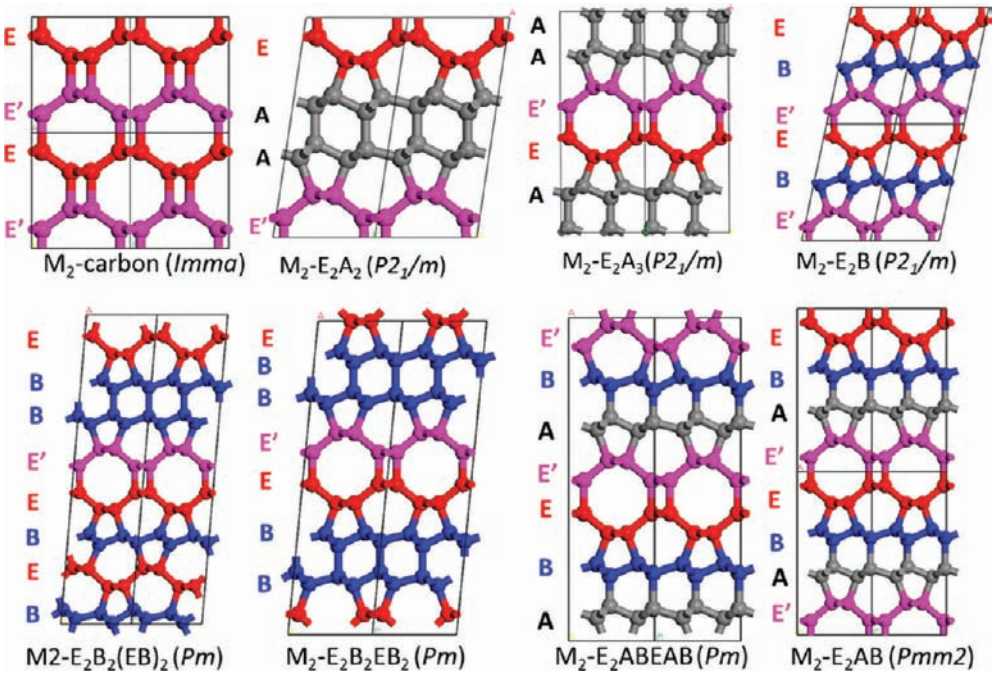

Figure 9. Eight handmade structures composed of A-type, B-type, E-type, and inversed E-type (or E′-type) buckled graphene layers. They are named according to the stacking sequence of the buckled graphene layers.

unbiased search), as shown in Figure 8b. The enhanced stability for Z-carbon-11 and Z-carbon-12 is largely due to added hexagonal-diamond fragmental layers in these two structures. The simulated XRD spectra of Z-carbon-11 and Z-carbon-12 (Figure 8c) appear to be in reasonable agreement with the experimental spectrum as well. Likewise, more A-type layers can be inserted into Z-carbon-2 or more B-type layers can be inserted into Z-carbon-3 to construct lower-energy structures composed of fragments of M-carbon and cubic-diamond.

It is also possible to construct structures belonging to a new group by stacking different combinations of buckled carbon layers. For example, stacking of double-E-layers (i.e., E and inversed E′ layer) can yield a new structure which contains tetrahedron/octahedron pairs. Since the E-type layers in this structure are found originally in M-carbon, we name this structure as M_2-carbon. With insertion of more A-type, B-type, and double-E-type layers into M_2-carbon, more carbon structures can be obtained. Eight handmade structures are shown in Figure 9. Among the eight, M_2-E_2A_2 and M_2-$E_2B_2EB_2$ are slightly lower in energy than M-carbon and the other six are all higher in energy than M-carbon.

■ CONCLUSION

In conclusion, on the basis of an unbiased search of crystalline structures of carbon using the evolutional algorithm, we attain nine new polymorphic phases of carbon besides the known crystalline structures reported in the literature. Analyzing the new polymorphic structures allows us to derive some generic structural features and trends for classifying low-energy sp^3-hybridized carbon structures. An important insight gained from this comprehensive study is that most low-energy sp^3-hybridized carbon structures can be classified into three groups, according to different ways of stacking two (or more) of the five (A−E) types of carbon layers. These five types of carbon layers can be viewed as different buckling of the graphene sheet in a periodic fashion. Another common feature in all nine structures predicted is that each stacking layer entails only one type of buckling. Hence, the transition barriers from graphite to these structures may not be so high due to closeness in layered carbon structure. Some of these structures may be synthesized by cold-compressing graphite. We also expect that crystalline structures with even lower energies can be found in future studies. Indeed, the generic structural classification obtained from this study allows us to construct new low-energy sp^3-hybridized carbon allotrope structures via stacking buckled graphene layers in different combination of the A−E types by design.

The calculated elastic moduli and hardness of several new crystalline structures are close to those of the cubic diamond. In particular, Z-carbon-4 possesses the highest hardness (93.4) among all the low-energy sp^3-hybridized carbon structures predicted today. The calculated wide electronic band gaps for many new structures are consistent with the observation that the cold-compressed graphite is optically transparent. All the results suggest that multiple crystalline structures may coexist in the experimental samples. The simulated XRD patterns support this speculation as well. To produce a single-crystal sample in experiments, one possible approach that may be tested in the laboratory is to make multiple heat treatments of the sample, followed by multiple annealing. The sample may still prefer to stay in the metastable polyamorphic state if the kinetics is extremely slow.

Note. When our paper was under review, we found that three preprints on cold-compressed carbon structures were posted on arXiv.org.[33] We note that the M10-carbon presented in ref 33a and the S-carbon presented in ref 33c are the same as the Z-carbon-1 presented in this work. Most structures reported in ref 33b, also obtained from evolutionary dynamics simulation, are composed of A-type to E-type buckled graphene layers, and some of these structures are the same as ours. In ref 33c, a different way to construct carbon allotropes is proposed, which is by inserting carbon zigzag chains into primitive

dx.doi.org/10.1021/ja301582d | J. Am. Chem. Soc. 2012, 134, 7530−7538

structures such as S-carbon and bct-C_4. Many structures constructed in this way however belong to new groups since they can be viewed as a stacking of buckled layers but with mixed buckling type A−E in each layer.

■ ASSOCIATED CONTENT

Supporting Information

Computed phonon spectra for the nine new crystalline structures of carbon. This material is available free of charge via the Internet at http://pubs.acs.org.

■ AUTHOR INFORMATION

Corresponding Author

xzeng1@unl.edu

Notes

The authors declare no competing financial interest.

■ ACKNOWLEDGMENTS

We thank Prof. Wendy Mao for sending us original XRD data of cold-compressed graphite. This work was supported by grants from the NSF (DMR-0820521) and ARL (W911NF1020099), by the Nebraska Research Initiative, and by the University of Nebraska's Holland Computing Center.

■ REFERENCES

(1) EI Goresy, A.; Donnay, G. *Science* **1968**, *161*, 363.

(2) EI Goresy, A.; Dubrovinsky, L. S.; Gillet, P.; Mostefaoui, S.; Graup, G.; Drakopoulos, M.; Simionovici, A. S.; Swamy, V.; Masaitis, V. L. *Geoscience* **2003**, *335*, 889.

(3) Ferroir, T.; Dubrovinsky, L.; Goresy, A. E.; Simionovici, A.; Nakamura, T.; Gillet, P. *Earth Planet. Sci. Lett.* **2010**, *290*, 150.

(4) Sumiya, H.; Irifune, T. *J. Mater. Res.* **2007**, *22*, 2345.

(5) Irifune, T.; Kurio, A.; Sakamoto, S.; Inoue, T.; Sumiya, H. *Nature* **2003**, *421*, 599.

(6) Bundy, F. P.; Kasper, J. S. *J. Chem. Phys.* **1967**, *46*, 3437.

(7) Patterson, J. R.; Catledge, S. A.; Vohra, Y. K.; Akella, J.; Weir, S. T. *Phys. Rev. Lett.* **2000**, *85*, 5364.

(8) Goncharov, A. F.; Makarenko, I. N.; Stishov, S. M. *J. Exp. Theor. Phys.* **1989**, *69*, 380.

(9) Hanfland, M.; Syassen, K.; Sonnenschein, R. *Phys. Rev. B* **1989**, *40*, 1951.

(10) Utsumi, W.; Yagi, T. *Science* **1991**, *252*, 1542.

(11) Mao, W. L.; Mao, H. K.; Eng, P. J.; Trainor, T. P.; Newville, M.; Kao, C.; Heinz, D. L.; Shu, J.; Meng, Y.; Hemley, R. J. *Science* **2003**, *302*, 425.

(12) Zhao, Y. X.; Spain, I. L. *Phys. Rev. B* **1989**, *40*, 993.

(13) Yagi, T.; Utsumi, W.; Yamakata, M.; Kikegawa, T.; Shimomura, O. *Phys. Rev. B* **1992**, *46*, 6031.

(14) Hanfland, M.; Beister, H.; Syassen, K. *Phys. Rev. B* **1989**, *39*, 12598.

(15) Xu, J.; Mao, H. K.; Hemley, R. J. *J. Phys.: Condens. Matter* **2002**, *14*, 11549.

(16) (a) Umemoto, K.; Wentzcovitch, R. M.; Saito, S.; Miyake, T. *Phys. Rev. Lett.* **2010**, *104*, 125504. (b) Zhou, X.-F.; Qian, G.-R.; Dong, X.; Zhang, L.; Tian, Y.; Wang, H.-T. *Phys. Rev. B* **2010**, *82*, 134126.

(17) Li, Q.; Ma, Y.; Oganov, A. R.; Wang, H.; Wang, H.; Xu, Y.; Cui, T.; Mao, H. K.; Zou, G. *Phys. Rev. Lett.* **2009**, *102*, 175506.

(18) (a) Wang, J.-T.; Chen, C.; Kawazoe, Y. *Phys. Rev. Lett.* **2011**, *106*, 075501. (b) Wang, J.-T.; Chen, C.; Kawazoe, Y. *Phys. Rev. B* **2011**, *84*, 012102.

(19) Pickard, C. J.; Needs, R. J. *Phys. Rev. B* **2010**, *81*, 014106.

(20) (a) Zhao, Z.; Xu, B.; Zhou, X.-F.; Wang, L.-M.; Wen, B.; He, J.; Liu, Z.; Wang, H. T.; Tian, Y. *Phys. Rev. Lett.* **2011**, *107*, 215502. (b) Selli, D.; Baburin, I. A.; Martoňák, R.; Leoni, S. *Phys. Rev. B* **2011**, *84*, 161411(R). (c) Amsler, M.; Flores-Livas, J. A.; Lehtovaara, L.; Balima, F.; Ghasemi, S. A.; Machon, D.; Pailhs, S.; Willand, A.; Caliste, D.; Botti, S.; Miguel, A. S.; Goedecker, S.; Marques, M. A. L. *Phys. Rev. Lett.* **2012**, *108*, 065501.

(21) (a) Oganov, A. R.; Lyakhov, A. O.; Valle, M. *Acc. Chem. Res.* **2011**, *44*, 227. (b) *Modern Methods of Crystal Structure Prediction*; Oganov, A. R., Ed., Wiley-VCH: Berlin, 2010.

(22) Luo, X.; Yang, J.; Liu, H; Wu, X.; Wang, Y.; Ma, Y.; Wei, S.; Gong, X.; Xiang, H. *J. Am. Chem. Soc.* **2011**, *133*, 16285.

(23) (a) Deaven, D. M.; Ho, K. M. *Phys. Rev. Lett.* **1995**, *75*, 288. (b) Back, T. *Evolutionary Algorithm in Theory and Practice: Evolutionary Programming, Genetic Algorithms*; Oxford University Press: Oxford, 1990.

(24) Kresse, G.; Furthmüller, J. *Phys. Rev. B* **1996**, *54*, 11169.

(25) Togo, A.; Oba, F.; Tanaka, I. *Phys. Rev. B* **2008**, *78*, 134106.

(26) Zhou, R.; Liu, R.; Li, L.; Wu., X.; Zeng, X. C. *J. Phys. Chem. C* **2011**, *115*, 18174.

(27) Šimůnek, A.; Vackář, J. *Phys. Rev. Lett.* **2006**, *96*, 085501.

(28) Segall, M.; Lindan, P.; Probert, M.; Pickard, C.; Hasnip, P.; Clark, S.; Payne, J. *J. Phys.: Condens. Matter* **2002**, *14*, 2717.

(29) Crespi, V. H.; Benedict, L. X.; Cohen, M. L.; Louie, S. G. *Phys. Rev B* **1996**, *53*, R13303.

(30) Terrones, H.; Terrones, M.; Hernández, E.; Grobert, N.; Charlier, J.-C.; Ajayan, P. M. *Phys. Rev. Lett.* **2000**, *84*, 1716.

(31) Rocquefelte, X.; Rignanese, G.-M.; Meunier, V.; Terrones, H.; Terrones, M.; Charlier, J.-C. *Nano Lett.* **2004**, *4*, 805.

(32) Lusk, M. T.; Carr, L. D. *Phys. Rev. Lett.* **2008**, *100*, 175503.

(33) (a) Amsler, M.; Flores-Livas, J. A.; Botti, S.; Marques, M. A. L.; Geodecker, S. *arXiv:1202.6030v1 [cond-mat.mtrl-sci]*. (b) Zhu, Q.; Zeng, Q.; Oganov. A. R. *arXiv:1203.0706v1 [cond-mat.mtrl-sci]*. (c) Niu, H.; Chen, X.-Q. Wang, S.; Li, D.; Mao, W. L.; Li, Y. *arXiv:1203.2998v1 [cond-mat.mtrl-sci]*.